Analytical Biochemistry 421 (2012) 699–705

Contents lists available at SciVerse ScienceDirect

Analytical Biochemistry

journal homepage: www.elsevier.com/locate/yabio

# Stable isotope liquid chromatography–tandem mass spectrometry assay for fatty acid amide hydrolase activity

Christin Rakers [a], Alexander A. Zoerner [a], Stefan Engeli [a], Sandor Batkai [a,b], Jens Jordan [a], Dimitrios Tsikas [a,*]

[a] Institute of Clinical Pharmacology, Hannover Medical School, 30623 Hannover, Germany
[b] Institute for Molecular and Translational Therapeutic Strategies, Hannover Medical School, 30623 Hannover, Germany

ARTICLE INFO

*Article history:*
Received 3 October 2011
Received in revised form 3 November 2011
Accepted 4 November 2011
Available online 13 November 2011

*Keywords:*
Anandamide
Endocannabinoids
Ethanolamine
FAAH
UPLC
HILIC

ABSTRACT

Fatty acid amide hydrolase (FAAH) is the main enzyme responsible for the hydrolysis of the endocannabinoid anandamide (arachidonoyl ethanolamide, AEA) to arachidonic acid (AA) and ethanolamine (EA). Published FAAH activity assays mostly employ radiolabeled anandamide or synthetic fluorogenic substrates. We report a stable isotope liquid chromatography–tandem mass spectrometry (LC–MS/MS) assay for specific, sensitive, and high-throughput capable FAAH activity measurements. The assay uses AEA labeled with deuterium on the EA moiety ($d_4$-AEA) as substrate and measures the specific reaction product tetradeutero-EA ($d_4$-EA) and the internal standard $^{13}C_2$-EA. Selected reaction monitoring of $m/z$ 66 → $m/z$ 48 ($d_4$-EA) and $m/z$ 64 → $m/z$ 46 ($^{13}C_2$-EA) in the positive electrospray ionization mode after liquid chromatographic separation on a HILIC (hydrophilic interaction liquid chromatography) column is performed. The assay was developed and thoroughly validated using recombinant human FAAH (rhFAAH) and then was applied to human blood and dog liver samples. rhFAAH-catalyzed $d_4$-AEA hydrolysis obeyed Michaelis–Menten kinetics ($K_M$ = 12.3 μM, $V_{max}$ = 27.6 nmol/min mg). Oleoyl oxazolopyridine (oloxa) was a potent, partial noncompetitive inhibitor of rhFAAH ($IC_{50}$ = 24.3 nM). Substrate specificity of other fatty acid ethanolamides decreased with decreasing length, number of double bonds, and lipophilicity of the fatty acid skeleton. In human whole blood, we detected FAAH activity that was inhibited by oloxa.



Fatty acid amide hydrolase (FAAH, EC 3.5.1.99)[1] degrades fatty acid amides, including bioactive lipid endocannabinoids. In vivo, FAAH hydrolyzes anandamide (arachidonoyl ethanolamide, AEA) to arachidonic acid (AA) and ethanolamine (EA) [1] (Fig. 1A). FAAH is widely distributed across the central nervous system and peripheral tissues. In human subjects, FAAH is predominantly expressed in pancreas, brain, and skeletal muscle [2]. FAAH knockout mice do not show major developmental or behavioral abnormalities [3]. Yet, these animals are pain insensitive [4]. Pharmacological FAAH inhibition increases fatty acid amide concentrations in various tissues. The intervention ameliorates pain and inflammation while inducing muscle relaxation [5,6]. FAAH activity may be altered in various diseases. Excessive FAAH activity may contribute to arterial hypertension in spontaneously hypertensive rats (SHRs) [7]. FAAH down-regulation in adipose tissue may contribute to peripheral endocannabinoid system activation in human obesity [8,9]. Decreased FAAH activity may also play a role in the pathogenesis of the neurodegenerative disorder Huntington's disease [10]. Determination of FAAH activity in biological samples is of particular importance in basic and clinical studies on the endocannabinoid system.

Published FAAH activity assays are often based on the use of radiolabeled AEA. Other assays rely on generation of fluorescent products from synthetic fluorogenic substances with little structural similarity to AEA [1,11]. The results from the latter assays might not fully reflect FAAH activity in biological samples. We developed an FAAH activity assay that runs under quasi-physiological conditions for the substrate AEA and the specific reaction product EA. However, EA is a ubiquitous molecule in many biological samples, resulting in high blank EA concentrations. Therefore, we applied deuterium-labeled AEA with the deuterium atoms located at the EA moiety. The reaction product deuterium-labeled EA can be measured by mass spectrometry (MS).

We decided to use the liquid chromatography (LC)–MS methodology because no extraction and derivatization steps are required. We report on the development, validation, and application of an

* Corresponding author. Fax: +49 511 532 2750.
*E-mail address:* tsikas.dimitros@mh-hannover.de (D. Tsikas).

[1] *Abbreviations used:* FAAH, fatty acid amide hydrolase; AEA, arachidonoyl ethan olamide (anandamide); AA, arachidonic acid; EA, ethanolamine; MS, mass spectrom etry; LC, liquid chromatography; MS/MS, tandem MS; oloxa, oleoyl oxazolopyridine; OEA, oleoyl ethanolamide; PEA, palmitoyl ethanolamide; oxy-AEA, oxy-arachidonoyl ethanolamide; $PGE_2$-EA, prostaglandin $E_2$ ethanolamide; virodhamine, arachidonic acid-(2-aminoethyl) ester; rhFAAH, recombinant human FAAH; HILIC, hydrophilic interaction liquid chromatography; ESI+, positive electrospray ionization; SRM, selected reaction monitoring; CID, collision-induced dissociation; EDTA, ethylenedi aminetetraacetic acid.

0003-2697/$ - see front matter © 2011 Elsevier Inc. All rights reserved.
doi:10.1016/j.ab.2011.11.003

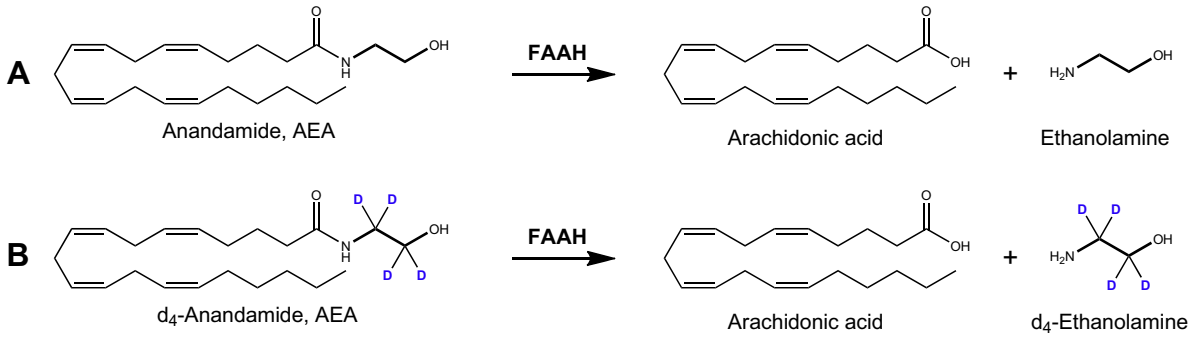


**Fig.1.** (A) In vivo, the enzyme FAAH hydrolyzes anandamide to EA and AA. (B) In the FAAH assay, the substrate tetradeutero-AEA ($d_4$-AEA) is hydrolyzed by FAAH to tetradeutero-ethanolamine ($d_4$-EA) and AA. FAAH activity is assessed by measuring $d_4$-EA formation by liquid chromatography–tandem mass spectrometry (LC–MS/MS) using $^{13}C_2$-EA as the internal standard.

LC–tandem MS (MS/MS) FAAH activity assay that uses a commercially available stable isotope-labeled AEA (fourfold deuterated, $d_4$-AEA). In this assay, FAAH-catalyzed hydrolysis of $d_4$-AEA yields deuterium-labeled ethanolamine ($d_4$-EA) (Fig. 1B), which is quantified by means of the stable isotope-labeled internal standard $^{13}C_2$-EA.

## Materials and methods

### *Chemicals*

*N*-(2-Hydroxyethyl-1,1,2,2-$^2H_4$)-5*Z*,8*Z*,11*Z*,14*Z*-eicosatetraenamide ($d_4$-AEA), *N*-(2-hydroxyethyl)-5*Z*,8*Z*,11*Z*,14*Z*-eicosatetraenamide-5,6,8,9,11,12,14,15-$^2H_8$) ($d_8$-AEA), oleoyl oxazolopyridine (olo xa, 1-oxazolo[4,5-b]pyridine-2-yl-octadec-9*Z*-en-1-one), oleoyl ethanolamide (OEA), palmitoyl ethanolamide (PEA), oxy-arachidonoyl ethanolamide (oxy-AEA), prostaglandin $E_2$ ethanolamide ($PGE_2$-EA), virodhamine [arachidonic acid-(2-aminoethyl ) ester] hydrochloride, and recombinant human FAAH (rhFAAH, supplied as a 30-mg protein/ml solution in 20 mM Hepes buffer, 425 U/ml) were purchased from Cayman Chemicals (Ann Arbor, MI, USA). 2-Amino[1,2-$^{13}C_2$]ethanol ($^{13}C_2$-EA) was obtained from Cambridge Isotope Laboratories (Andover, MA, USA). AM404 [(5*Z*,8*Z*,11*Z*,14*Z*)-*N*-(4-hydroxyphenyl)icosa-5,8,11,14-tetraenamide] was obtained from Tocris (Ellisville, MO, USA), LC–MS-grade acetonitrile was supplied by Honeywell (Seelze, Germany). LC–MS-grade water was generated by a Milli-Q water purification system (Millipore, Billerica, MA, USA). LC–MS-grade ammonium formate and formic acid were purchased from Sigma–Aldrich (Munich, Germany). Dog liver tissue was kindly donated for research purposes by the Hannover Veterinary School. The concentration of stable isotope-labeled analytes in their stock solutions was standardized by using stock solutions of their accurately weighed unlabeled analogues.

### *LC–MS/MS conditions*

LC–MS/MS analyses were performed on a quadrupole tandem mass spectrometer Xevo TQ MS coupled to an ACQUITY UPLC (ultra-performance liquid chromatography) system from Waters (Eschborn, Germany). A ZIC-HILIC (hydrophilic interaction liquid chromatography) HPLC (high-performance liquid chromatography) column (100 × 2.1 mm i.d., 3.5 μm particle size) from Merck (Darmstadt, Germany) was used and operated at 25 °C. Isocratic elution at a constant flow rate of 0.2 ml/min was performed. The mobile phase consisted of 25 mM ammonium formate in water containing 0.1% formic acid (w/v) and acetonitrile (1:1, v/v). The autosampler was thermostated at 5 °C. Sample aliquots of 1 μl were injected into the system using the partial loop mode. LC–MS/MS analyses were carried out in positive electrospray ionization mode (ESI+). Desolvation gas temperature, desolvation gas flow rate, and capillary voltage were 600 °C, 1000 L/h, and 0.5 kV, respectively. Quantification was performed by selected reaction monitoring (SRM) of the transitions $m/z$ 62.0 → 44.0 for $d_0$-EA, $m/z$ 66.0 → 48.1 for $d_4$-EA, $m/z$ 64.0 → 46.1 for $^{13}C_2$-EA, $m/z$ 348.4 → 62.0 for $d_0$-AEA, $m/z$ 352.4 → 66.0 for $d_4$-AEA, and $m/z$ 356.4 → 62.0 for $d_8$-AEA. Argon was used as collision gas for collision-induced dissociation (CID). Collision energy was set to 14 eV for EA and 7 eV for AEA; cone voltage was 18 V for EA and 22 V for AEA. Injected amounts of analytes (A) and their internal standard (IS) are directly proportional to their concentrations in the biological sample and to their peak areas measured. Thus, $d_4$-AEA and $d_4$-EA concentrations ($C_A$) were calculated by multiplying the peak area ($PA$) ratio of measured peak areas of analyte ($PA_A$) and internal standard ($PA_{IS}$) by the known concentration of the respective internal standard concentration ($C_{IS}$): $C_A = C_{IS} \times PA_A/PA_{IS}$.

### *General remarks about the LC–MS/MS FAAH assay*

Assays were performed at room temperature (20–23 °C) or at 37 °C as specified. Total sample volume was always 100 μl of 10 mM potassium phosphate buffer (pH 7.3) in glass vials that were shaken gently. If not otherwise specified, 0.1 U of FAAH was used. Reaction was started by adding the substrate $d_4$-AEA (28 μM in ethanol) to sample to reach a final concentration of 1 μM or as specified. Reaction was terminated after an appropriate time by using various protein precipitation procedures, including acidification by HCl acid, treatment with acetonitrile (1:1, v/v), and addition of the FAAH inhibitor oloxa as specified. $^{13}C_2$-EA (160 μM in water) was added to the samples at a fixed final concentration of 1.6 μM and served as internal standard for $d_4$-EA quantification. All procedures deviating from those described above are specified in the respective experiments in the Results and Discussion sections.

All analyses were performed in duplicate in two independent experiments if not otherwise specified. GraphPad Prism 5 from GraphPad Software (La Jolla, CA, USA) was used for data analysis. $K_M$ and $V_{max}$ values were calculated based on the Michaelis–Menten equation by nonlinear regression. Data are presented as means ± standard errors.

### *Preparation of dog liver protein microsomes*

Dog liver samples (2 g) were portioned to approximately 100-mg pieces that were then stored at −70 °C. Frozen liver pieces were homogenized in 50 mM Hepes containing 1 mM

ethylenediaminetetraacetic acid (EDTA) and 5 μl/ml of a protease inhibitor mixture by means of a Precellys 24 dual homogenizer (Bertin Technologies, Montigny le Bretonneux, France) equipped with a Cryolysis cooling device at 5 °C (two times for 25 s at 5500 rpm). Homogenates were pooled and centrifuged (20 min, 20,000*g*, 4 °C). The supernatant was centrifuged (60 min, 100,000*g*, 4 °C), and the pellet (microsomes fraction) was resuspended in 4 ml of buffer and stored at −70 °C. The final liver protein concentration was determined to be 6.9 mg/ml by using a commercially available BCA (bisinchoninic acid) protein assay kit (Thermo Scientific, Rockford, IL, USA).

## Results

### *Analytical performance of LC–MS/MS method*

Unlabeled and labeled AEA and EA eluted as symmetric peaks at 1.15 and 2.52 min, respectively, with a peak width at baseline of approximately 25 s each. Total analysis time was 4 min (see below; see also Fig. S1 in Supplementary material).

The most intense ions in the MS ESI+ spectra of $d_4$-EA and $^{13}C_2$-EA were *m/z* 66 and 64, respectively (Figs. 2A and 2B). The most intense ion in the MS ESI+ spectrum of unlabeled EA was *m/z* 62 (not shown). These ions represent the protonated molecules $[M+H]^+$. Less intense ions were detected at *m/z* 46 for $^{13}C_2$-EA (Fig. 2B), *m/z* 48 for $d_4$-EA (Fig. 2A), and *m/z* 44 for unlabeled EA (not shown). These ions most likely result from neutral loss of water (18 Th) due to in-source fragmentation of $[M+H]^+$.

MS/MS ESI+ spectra were generated by CID of $[M+H]^+$ with argon. The MS/MS ESI+ spectra of $d_4$-EA (Fig. 2C) and $^{13}C_2$-EA (Fig. 2D) are very similar to the MS ESI+ spectra of these analytes. The intensity of the product ions was higher and depended on the extent of the collision energy (data not shown). Interestingly, and in contrast to the MS ESI+ spectra, the product ion spectra contained minor ions at *m/z* 49 for $d_4$-EA (Fig. 2C), *m/z* 47 for $^{13}C_2$-EA (Fig. 2D), and *m/z* 45 for unlabeled EA (not shown). These ions are most likely produced by CID-neutral loss of ammonia (17 Th) from $[M+H]^+$. Thus, CID of EA in ESI+ seems to produce protonated cyclo-aminoethane and ethylene oxide.

Based on these results, the following SRM was used in quantitative analyses: *m/z* 66 → 48 for $d_4$-EA and *m/z* 64 → 46 for $^{13}C_2$-EA. In some analyses, the transition *m/z* 62 → 44 for unlabeled EA was used in addition. Furthermore, in selected analyses, the mass transitions *m/z* 348 → 62 for $d_0$-AEA, *m/z* 352 → 66 for $d_4$-AEA, and *m/z* 356 → 62 for $d_8$-AEA were used as described previously [12].

The limit of detection, defined as the lowest amount of the internal standard $^{13}C_2$-EA injected into the LC–MS/MS system that resulted in a peak with a signal-to-noise ratio of 3:1, was determined to be 128 fg (2 fmol).

Standard curves were prepared by LC–MS/MS in the concentration range of 0 to 2 μM for $d_4$-EA using the internal standard $^{13}C_2$-EA at a fixed concentration of 1.6 μM. Regression analysis between the peak area ratio of *m/z* 48 (from *m/z* 66) for $d_4$-EA to *m/z* 46 (from *m/z* 64 for $^{13}C_2$-EA) (*y*) and the concentration of $^{13}C_2$-EA (*x*) resulted in the regression equation $y = 0.01 + 0.625x$ ($r^2 = 0.999$, $P < 0.0001$). The imprecision (relative standard deviation) in these analyses ranged between 0.1 and 2%.

### *Assay characterization using rhFAAH*

#### *Stoichiometry*

rhFAAH-catalyzed hydrolysis of $d_4$-AEA (1.5 μM) and formation of $d_4$-EA from $d_4$-AEA were monitored simultaneously over time (range = 0–30 min) at 37 °C. FAAH reaction was terminated after the respective incubation time by adding 100-μl aliquots of ice-cooled acetonitrile containing the internal standards $d_8$-AEA (225 nM) and $^{13}C_2$-EA (1.6 μM) and by immediate centrifugation (5 min, 4600 rpm, 4 °C). Aliquots (100 μl) of the supernatants were transferred into glass vials, from which 1-μl aliquots were injected into the LC–MS/MS system and analyzed for $d_4$-AEA and $d_4$-EA by

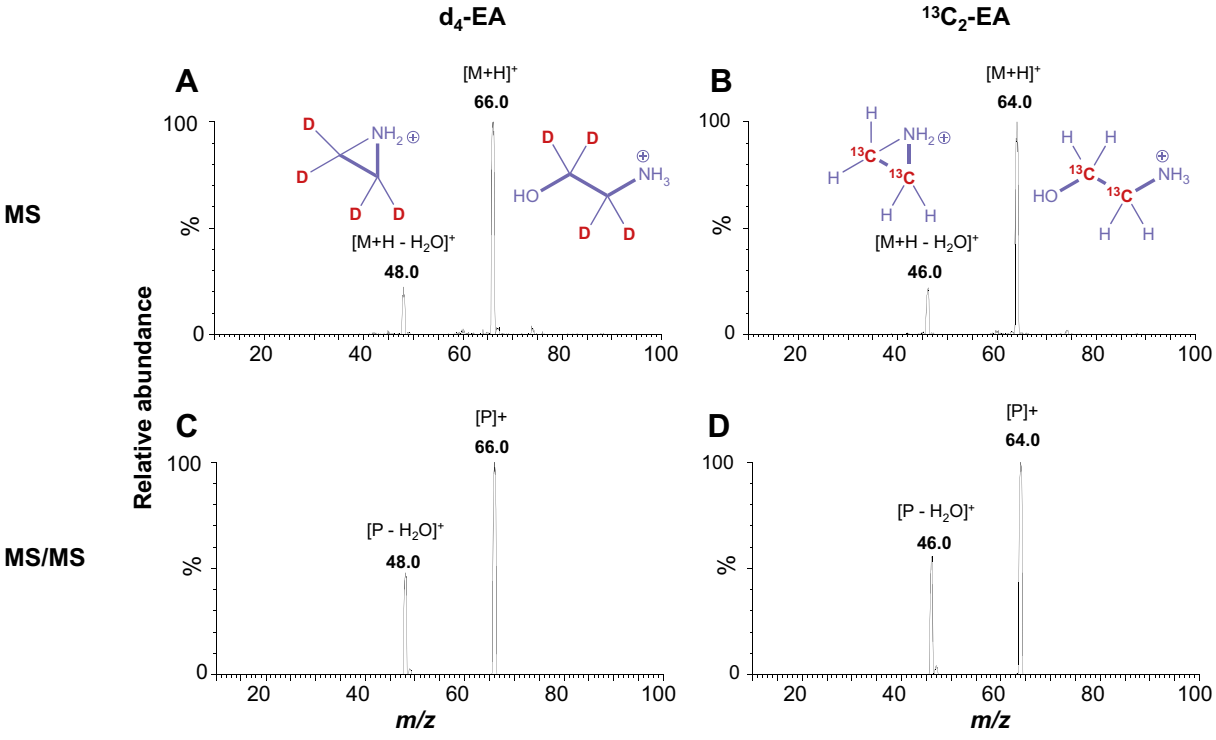


**Fig.2.** MS (A, B) and MS/MS (C, D) ESI+ spectra of $d_4$-EA and its internal standard $^{13}C_2$-EA. Data were obtained in the range of *m/z* 10 to 100 with a rate of 0.5 scans per second after injection of 1 ng of $d_4$-EA and $^{13}C_2$-EA each on a HILIC column. Asterisks indicate the $^{13}C$ label. Insets illustrate the structure of parent (P, $[M+H]^+$) and product ions.

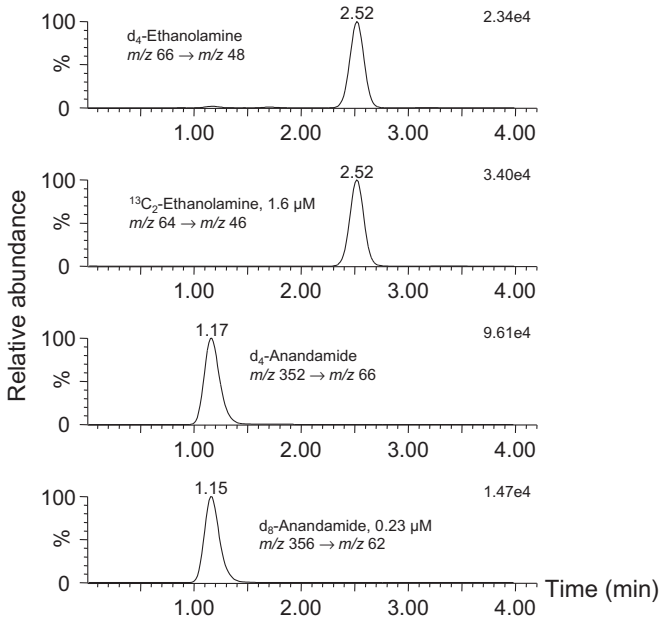


**Fig.3.** Typical LC–MS/MS chromatograms obtained from the analysis of a 1-µl aliquot of an rhFAAH assay mixture after incubation of $d_4$-AEA (1.6 µM) for 12 min at 37 °C. The concentrations of the internal standards were 1.6 µM for $^{13}C_2$-EA and 230 nM for $d_8$-AEA.

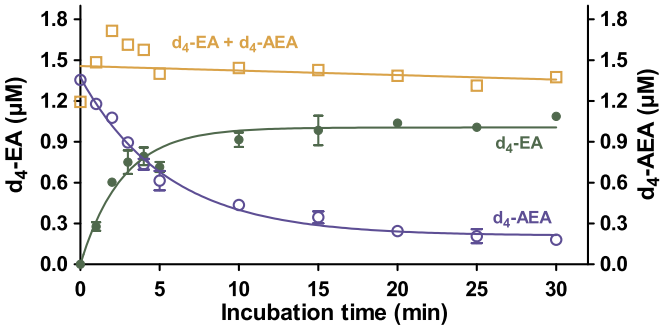


**Fig.4.** FAAH-catalyzed hydrolysis of $d_4$-AEA and formation of $d_4$-EA at 37 °C over incubation time. rhFAAH (0.1 U) was incubated with $d_4$-AEA (1.5 µM). FAAH reaction was terminated at the indicated time points by adding acetonitrile (1:1, v/v). Concentrations of $d_4$-AEA and $d_4$-EA were determined simultaneously by LC–MS/MS. Data were analyzed by nonlinear regression.

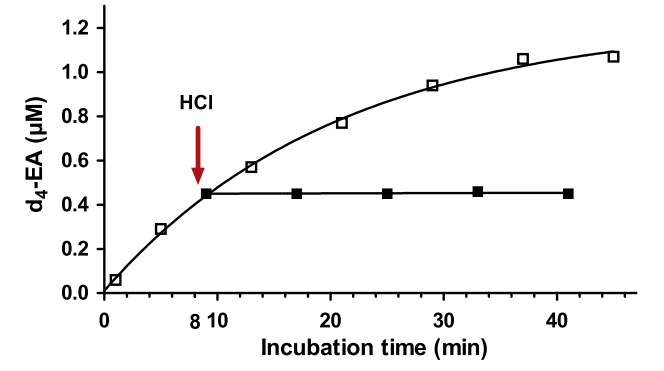


**Fig.5.** Measured $d_4$-EA concentrations from rhFAAH-catalyzed hydrolysis of $d_4$-AEA (1.5 µM) at 22 °C. After 8 min of incubation, the sample was split into two samples of equal volume. To one of these samples, 2 µl of a 1.2-M HCl solution was added (arrow, solid square symbols). The second sample was left unaltered (cross symbols). Alternating measurements were performed for the next 32 min. $r^2$ was 0.997 for nonlinear simulation.

SRM. Fig. S1 and Fig. 3 show typical chromatograms from analyses of $d_4$-AEA and $d_4$-EA in a standard mixture and in an FAAH assay mixture, respectively. Fig. 4 shows that decay of $d_4$-AEA and formation of $d_4$-EA occur in a stoichiometric manner. The sum of $d_4$-EA and $d_4$-AEA concentration was virtually constant and of the order of the initially added $d_4$-AEA concentration in this experiment. Indeed, under similar conditions but in the absence of FAAH, $d_4$-AEA was stable over 30 min and no $d_4$-EA was detectable in the sample. These findings suggest that both $d_4$-AEA and $d_4$-EA are chemically stable under the conditions used in the study and that potential ion suppression due to the short retention time of AEA did not affect its quantitative analysis.

*Linearity*

Fig. 5 shows that $d_4$-EA concentration increases linearly with incubation time up to approximately 12 min. Sample acidification by HCl acid stopped FAAH-catalyzed $d_4$-EA formation from $d_4$-AEA. Addition of either oloxa (1 µM), phenylmethanesulfonyl fluoride (PMSF, 10 µM), or URB597 (1 µM) terminated the FAAH reaction (data not shown).

*pH dependence of FAAH activity*

In potassium acetate buffer (pH 4.0 and 5.0), rhFAAH activity was 0.5 nmol/min mg rhFAAH (see Fig. S2 in Supplementary material). With increasing pH, FAAH activity increased as well. At the highest pH tested (8.0), FAAH activity was 3.0 nmol/min mg rhFAAH. The working pH value was 7.3 in all subsequent experiments.

*Michaelis–Menten kinetics of $d_4$-AEA hydrolysis through rhFAAH*

All experiments in this series were performed with rhFAAH (0.1 U) in 100-µl aliquots of 10 mM phosphate buffer (pH 7.3) at 37 °C. Incubation time was 5 min, and $d_4$-AEA concentration was between 0.25 and 40 µM. Reaction was stopped by adding 2 µl of a 1.2-M HCl solution. FAAH activity was calculated from measured $d_4$-EA concentrations using $^{13}C_2$-EA (1.59 µM). Fig. 6 shows that rhFAAH-catalyzed hydrolysis of $d_4$-AEA to $d_4$-EA obeys the Michaelis–Menten kinetics with $K_M = 12.3 \pm 1.6$ µM and $V_{max} = 27.6 \pm 1.73$ nmol $d_4$-EA/min mg FAAH.

*rhFAAH inhibition by oloxa*

The effect and kinetics of the known FAAH inhibitor oloxa [13] on rhFAAH activity were investigated for varying concentrations of $d_4$-AEA (0.25, 0.5, 1, 2, 4, 20, and 40 µM) and of oloxa (0, 1, 10, and 50 nM). After preincubation of rhFAAH (0.1 U) in 10 mM phosphate buffer (pH 7.3) with oloxa for 5 min at 37 °C, reaction was initiated by adding $d_4$-AEA to the samples. After an incubation time of 5 min at 37 °C, FAAH activity was stopped by HCl acidification. The results shown in Fig. 7 indicate that oloxa is a partial noncompetitive inhibitor of rhFAAH.

For $IC_{50}$ value determination for oloxa, rhFAAH (0.1 U) was preincubated with varying oloxa concentrations (1, 2, 5, 10, 15, 20, 50, 100, 200, and 500 nM) for 10 min at 37 °C. The reaction was started by adding $d_4$-AEA at a final concentration of 1.5 µM. After 5 min of incubation at 37 °C, the reaction was terminated by adding acetonitrile (1:1, v/v). Percentage rhFAAH activity inhibition by oloxa was calculated and plotted against the oloxa concentration. Fig. 8 shows a sigmoidal dose–response curve. The $IC_{50}$ value of oloxa was determined to be 24.3 nM.

*Evaluation of selected substances as inhibitors and substrates for rhFAAH*

LC–MS/MS assays with rhFAAH were used to investigate substrate specificity. The compounds tested were the fatty acid

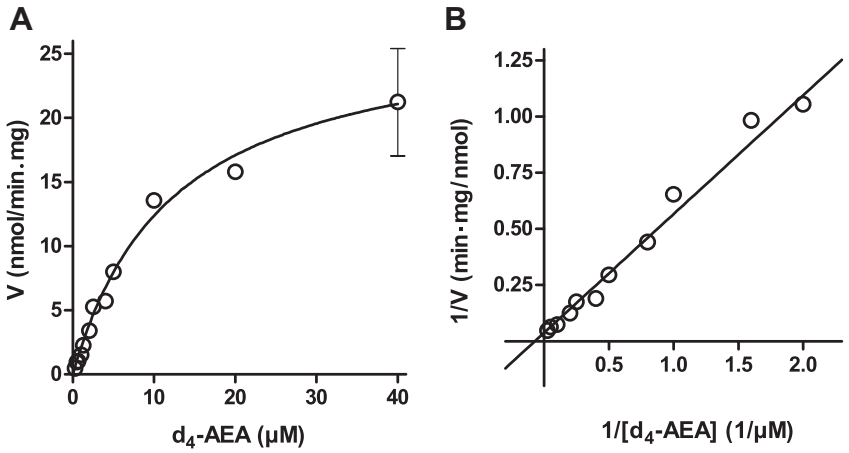


**Fig.6.** rhFAAH-catalyzed hydrolysis of $d_4$-AEA to $d_4$-EA: (A) direct plot; (B) Lineweaver–Burk plot. Symbols indicate measured values (means ± standard errors, $n = 2$), and lines indicate the computer simulation of the data for Michaelis–Menten kinetics ($r^2 = 0.959$ for the direct plot, $r^2 = 0.994$ for the Lineweaver–Burk plot).

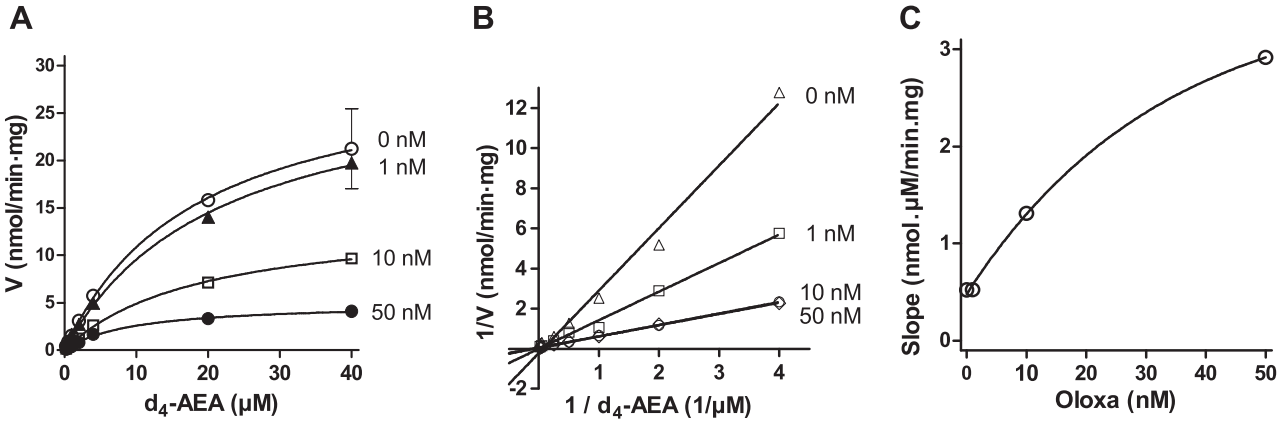


**Fig.7.** Inhibition of rhFAAH activity by oloxa: (A) direct plot; (B) Lineweaver–Burk plot; (C) secondary plot. $d_4$-AEA concentrations were 0.25, 0.5, 1, 2, 4, 20, and 40 μM. Oloxa concentrations were 0, 1, 10, and 50 nM. Data are shown as means ± standard errors from two independent experiments performed in 10 mM phosphate buffer (pH 7.3) at 37 °C using 0.1 U of rhFAAH. Preincubation and incubation time was 5 min each. $r^2$ values were better than 0.989 for nonlinear (A, C) and linear (B) regression analysis.

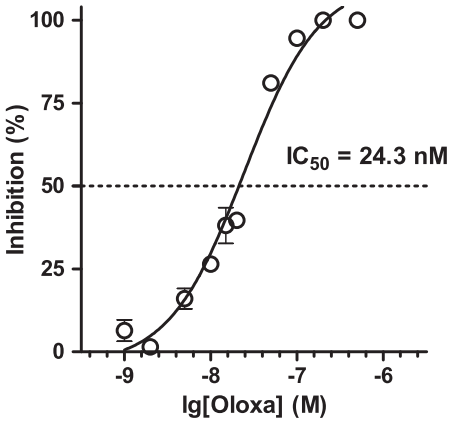


**Fig.8.** rhFAAH inhibition by oloxa. rhFAAH (0.1 U) was incubated with varying concentrations of oloxa (1–500 nM) for 5 min at 37 °C following a preincubation time of 10 min. Data are shown as means ± standard errors from two independent experiments.

ethanol amides OEA and PEA, $PGE_2$-EA, and virodhamine (see Fig. S3 in Supplementary material). OEA and PEA were found to be good substrates for rhFAAH, unlike $PGE_2$-EA and virodhamine.

**Table 1**
Determined enzyme kinetic parameters for FAAH from various sources.

| FAAH source | $K_M$ (μM) | $V_{max}$ (nmol/min mg protein) |
|---|---|---|
| Human recombinant | 12.3 | 27.6 |
| Human liver cytosol | Not applicable | Not detectable |
| Human liver mitochondria | 3.3 | 0.6 |
| Human liver microsomes | 2.4 | 1.4 |
| Dog liver microsomes | 1.8 | 4.8 |

The substrate specificity order was as follows: AEA ≈ OEA > PEA >> $PGE_2$-EA ≈ virodhamine (Fig. S3).

*FAAH activity in human and dog liver fractions and in human whole blood*

FAAH activity was measured in commercially available human liver fractions (cytosol, mitochondria, and microsomes). These fractions were diluted with 10 mM phosphate buffer (pH 7.3) to a protein concentration of 5 μg/ml. FAAH activity was also assessed in microsomes isolated from dog liver by standard centrifugation techniques. Protein concentration was adjusted between 5 and 60 μg/ml in dog liver microsomes. The highest FAAH activity in liver was measured in microsomes from human and dog liver, whereas no FAAH activity was found in human liver cytosol

(Table 1). Oloxa (at 50 nM) almost completely inhibited $d_4$-EA formation from $d_4$-AEA in human and dog liver microsomes (data not shown).

FAAH activity in human whole blood was detected by incubating $d_4$-AEA (1.6 μM) and the internal standard in whole blood (2 ml) for 10 min. The reaction was terminated by centrifugation in the cold (4 °C). Plasma proteins were precipitated by mixing plasma (0.5 ml) with acetonitrile (0.5 ml) that contained the internal standard $^{13}C_2$-EA. After centrifugation, 1-μl aliquots of the supernatant were analyzed by LC–MS/MS for $d_4$-AEA. In freshly obtained EDTA blood from six healthy volunteers, we detected low FAAH activity on the order of 6 pmol/min. $d_4$-EA formation from $d_4$-AEA in whole blood was inhibited by oloxa ($IC_{50}$, 500 nM). The 20-fold higher $IC_{50}$ value for oloxa in human whole blood compared with rhFAAH is likely due to the high protein binding of this drug.

*rhFAAH-catalyzed formation of anandamide from AA and EA*

The ability of FAAH to catalyze $d_4$-AEA synthesis from AA and $d_4$-EA was investigated by incubating rhFAAH (0.1 U) with AA (10 or 1000 μM) and $d_4$-EA (10 or 1000 μM) in 10 mM phosphate buffer (pH 7.3) for 30 min at 37 °C. The reaction was stopped by adding acetonitrile (1:1, v/v) containing $^{13}C_2$-EA. Control samples contained AA and $d_4$-EA but not rhFAAH. We observed rhFAAH-catalyzed formation of $d_4$-AEA at both AA and $d_4$-EA concentrations. Yet, the yield of $d_4$-AEA was on the order of 0.01% each (data not shown), suggesting that the main function of FAAH is anandamide hydrolysis rather than its synthesis from AA and EA.

## Discussion

A rational approach of determining FAAH enzyme activity is to measure the formation of the physiological reaction products AA and EA. However, AA and EA are ubiquitously present in biological samples and originate from multiple sources. Thus, the small AA and EA quantities produced by FAAH in vitro might not be reliably detectable in the presence of large background concentrations. To overcome this difficulty, radiolabeled fatty acid ethanolamides such as $^3$H-AEA and $^{14}$C-AEA [14,15] have been employed in FAAH activity assays. The radiolabeled reaction products EA and AA are separated by chromatography or charcoal adsorption, and radioactivity of the collected fractions is counted. Here, we reported on an alternative FAAH assay that uses AEA labeled in the ethanolamide moiety with deuterium ($d_4$-AEA) as the substrate and measures the FAAH-specific deuterium-labeled reaction product ethanolamine ($d_4$-AEA) by LC–MS/MS in the ESI+ mode. The only required sample treatment procedure is protein precipitation for enzyme inactivation. Protein precipitation using HCl acid or acetonitrile was equally effective and well-suited for LC–MS/MS analyses. In contrast to gas chromatography (GC)- and LC-based methods for EA analysis [16–18], in the current LC–MS/MS FAAH assay no derivatization is needed because HILIC is highly compatible with MS. HILIC allows for rapid isocratic chromatographic separation of highly hydrophilic analytes such as EA from highly lipophilic analytes such as anandamide. Furthermore, common mobile phases such as ammonium formate/acetonitrile mixtures acidified by formic acid can be used.

In the current LC–MS/MS assay, total analysis time was only 4 min, allowing for high-throughput analysis. However, anandamide adsorption on plastic materials and binding to proteins in the assay mixture may limit application of the current LC–MS/MS FAAH activity assay in high-throughput mode (see Fig. S4 in Supplementary material). Use of glass vials or addition of Tween 20 overcomes anandamide loss through adsorption on plastic material. Proteins at low concentrations as used in our experiments with rhFAAH do not compromise high-throughput analysis and could be used for screening of potential FAAH inhibitors and substrates.

The strong amine EA is entirely protonated under the chosen LC conditions. ESI+ yields protonated EA molecules $[M+H]^+$ at high yield, which seem to spontaneously lose water during the ionization process. EA does not form adducts with $Na^+$ or $K^+$. However, $[M+H]^+$ of EA seems to be quite stable under CID conditions, analogous to the $Na^+$ or $K^+$ adducts of anandamide [12]. Remarkably, $[M+H-H_2O]^+$ formation in the ion-source seems to occur more readily than $[M+H-H_2O]^+$ product ion formation in the collision chamber of the LC–MS/MS apparatus under ESI+ conditions.

First, we thoroughly developed and validated a novel LC–MS/MS assay using a commercially available rhFAAH enzyme preparation. Then, we applied the assay to measure FAAH activity in commercially available human liver fractions (cytosol, mitochondria, and microsomes) and newly prepared dog liver microsomes. We slightly modified the procedure to detect and quantify FAAH activity in fresh whole blood from healthy volunteers. FAAH-catalyzed hydrolysis of $d_4$-AEA to $d_4$-EA obeyed the Michaelis–Menten kinetics. $K_M$ was in the range of 2 to 12 μM. This $K_M$ value range is approximately three orders of magnitude higher than the physiological concentration of anandamide in human plasma and tissue [19]. Reported $K_M$ values for FAAH-catalyzed hydrolysis of AEA range between 0.8 and 180 μM [1,11,20–22]. The previously reported pH optimum of the FAAH-catalyzed reaction is approximately 8.0 to 9.0 [20,23,24]. Our results support these findings.

Virodhamine is structurally related to AEA. The molecule is an EA ester but not an EA amide derivative of AA. FAAH may possess esterase activity in addition to its amidase activity. Indeed, FAAH hydrolyzes the endocannabinoid 2-arachidonoyl glycerol (2-AG) [25]. This finding is supported by our observations on virodhamine. Yet, fatty acid ethanol amides are by far the preferred FAAH substrates.

Our results show that oloxa is a potent partial noncompetitive rhFAAH inhibitor at $IC_{50}$ = 24 nM. This value is approximately 10 times higher than the $IC_{50}$ value of 2.3 nM reported for rat liver plasma membrane extracts using radiolabeled oleamide rather than OEA as FAAH substrate [13].

In conclusion, we have developed a novel FAAH activity assay using the specific FAAH substrate $d_4$-AEA. The LC–MS/MS method is a useful assay to reliably assess FAAH activity in various biological samples. We will apply the methodology in pathophysiological studies on human disorders that may be associated with altered FAAH activity such as obesity and arterial hypertension [8,9]. Moreover, the assay can be applied to screen potential FAAH substrates and inhibitors. The issue is relevant because FAAH inhibitors undergo preclinical and clinical development for the treatment of pain and inflammatory diseases [26].

## Acknowledgment

S.B. acknowledges support from the Alexander von Humboldt Foundation and the European Commission (FP7- CIG- 294278).

## Appendix A. Supplementary data

Supplementary data associated with this article can be found, in the online version, at doi:10.1016/j.ab.2011.11.003.

## References

[1] C.J. Fowler, K.O. Jonsson, G. Tiger, Fatty acid amide hydrolase: biochemistry, pharmacology, and therapeutic possibilities for an enzyme hydrolyzing anandamide, 2-arachidonoylglycerol, palmitoylethanolamide, and oleamide, Biochem. Pharmacol. 62 (2001) 517–526.
[2] D.K. Giang, B.F. Cravatt, Molecular characterization of human and mouse fatty acid amide hydrolases, Proc. Nat. Acad. Sci. U.S.A. 94 (1997) 2238–2242.

[3] P. Pacher, S. Batkai, D. Osei-Hyiaman, L. Offertaler, J. Liu, J. Harvey-White, A. Brassai, Z. Jarai, B.F. Cravatt, G. Kunos, Hemodynamic profile, responsiveness to anandamide, and baroreflex sensitivity of mice lacking fatty acid amide hydrolase, Am. J. Physiol. Heart Circ. Physiol. 289 (2005) H533–H541.
[4] A.H. Lichtman, C.C. Shelton, T. Advani, B.F. Cravatt, Mice lacking fatty acid amide hydrolase exhibit a cannabinoid receptor-mediated phenotypic hypoalgesia, Pain 109 (2004) 319–327.
[5] S. Holt, F. Comelli, B. Costa, C.J. Fowler, Inhibitors of fatty acid amide hydrolase reduce carrageenan-induced hind paw inflammation in pentobarbital-treated mice: comparison with indomethacin and possible involvement of cannabinoid receptors, Br. J. Pharmacol. 146 (2005) 467–476.
[6] K. Ahn, D.S. Johnson, M. Mileni, D. Beidler, J.Z. Long, M.K. McKinney, E. Weerapana, N. Sadagopan, M. Liimatta, S.E. Smith, S. Lazerwith, C. Stiff, S. Kamtekar, K. Bhattacharya, Y. Zhang, S. Swaney, B.K. Van, R.C. Stevens, B.F. Cravatt, Discovery and characterization of a highly selective FAAH inhibitor that reduces inflammatory pain, Chem. Biol. 16 (2009) 411–420.
[7] S. Batkai, P. Pacher, D. Osei-Hyiaman, S. Radaeva, J. Liu, J. Harvey-White, L. Offertaler, K. Mackie, M.A. Rudd, R.D. Bukoski, G. Kunos, Endocannabinoids acting at cannabinoid-1 receptors regulate cardiovascular function in hypertension, Circulation 110 (2004) 1996–2002.
[8] S. Engeli, J. Bohnke, M. Feldpausch, K. Gorzelniak, J. Janke, S. Batkai, P. Pacher, J. Harvey-White, F.C. Luft, A.M. Sharma, J. Jordan, Activation of the peripheral endocannabinoid system in human obesity, Diabetes 54 (2005) 2838–2843.
[9] M. Bluher, S. Engeli, N. Kloting, J. Berndt, M. Fasshauer, S. Batkai, P. Pacher, M.R. Schon, J. Jordan, M. Stumvoll, Dysregulation of the peripheral and adipose tissue endocannabinoid system in human abdominal obesity, Diabetes 55 (2006) 3053–3060.
[10] N. Battista, M. Bari, A. Tarditi, C. Mariotti, A.C. Bachoud-Levi, C. Zuccato, A. Finazzi-Agro, S. Genitrini, M. Peschanski, S. Di Donato, E. Cattaneo, M. Maccarrone, Severe deficiency of the fatty acid amide hydrolase (FAAH) activity segregates with the Huntington's disease mutation in peripheral lymphocytes, Neurobiol. Dis. 27 (2007) 108–116.
[11] M.K. Ramarao, E.A. Murphy, M.W. Shen, Y. Wang, K.N. Bushell, N. Huang, N. Pan, C. Williams, J.D. Clark, A fluorescence-based assay for fatty acid amide hydrolase compatible with high-throughput screening, Anal. Biochem. 343 (2005) 143–151.
[12] A.A. Zoerner, S. Batkai, M.T. Suchy, F.M. Gutzki, S. Engeli, J. Jordan, D. Tsikas, Simultaneous UPLC–MS/MS quantification of the endocannabinoids 2-arachidonoyl glycerol (2AG), 1-arachidonoyl glycerol (1AG), and anandamide in human plasma: Minimization of matrix effects, 2AG/1AG isomerization, and degradation by toluene solvent extraction, J. Chromatogr. B (in press) doi:10.1016/j.jchromb.2011.06.025.
[13] D.L. Boger, H. Sato, A.E. Lerner, M.P. Hedrick, R.A. Fecik, H. Miyauchi, G.D. Wilkie, B.J. Austin, M.P. Patricelli, B.F. Cravatt, Exceptionally potent inhibitors of fatty acid amide hydrolase: the enzyme responsible for degradation of endogenous oleamide and anandamide, Proc. Nat. Acad. Sci. U.S.A. 97 (2000) 5044–5049.
[14] D.G. Deutsch, S.A. Chin, Enzymatic synthesis and degradation of anandamide, a cannabinoid receptor agonist, Biochem. Pharmacol. 46 (1993) 791–796.
[15] M. Maccarrone, M. Bari, A.F. Agro, A sensitive and specific radiochromatographic assay of fatty acid amide hydrolase activity, Anal. Biochem. 267 (1999) 314–318.
[16] O. Mrklas, A. Chu, S. Lunn, Determination of ethanolamine, ethylene glycol, and triethylene glycol by ion chromatography for laboratory and field biodegradation studies, J. Environ. Monit. 5 (2003) 336–340.
[17] K. Guo, L. Li, Differential$^{12}$C-/$^{13}$C-isotope dansylation labeling and fast liquid chromatography/mass spectrometry for absolute and relative quantification of the metabolome, Anal. Chem. 81 (2009) 3919–3932.
[18] S. Spanner, G.B. Ansell, The determination of free ethanolamine in brain tissue and its release on incubation, J. Neurochem. 30 (1978) 497–498.
[19] A.A. Zoerner, F.M. Gutzki, S. Batkai, M. May, C. Rakers, S. Engeli, J. Jordan, D. Tsikas, Quantification of endocannabinoids in biological systems by chromatography and mass spectrometry: a comprehensive review from an analytical and biological perspective, Biochim. Biophys. Acta 1811 (2011) 706–723.
[20] C.J. Hillard, D.M. Wilkison, W.S. Edgemond, W.B. Campbell, Characterization of the kinetics and distribution of *N*-arachidonylethanolamine (anandamide) hydrolysis by rat brain, Biochim. Biophys. Acta 1257 (1995) 249–256.
[21] S. Maurelli, T. Bisogno, L. De Petrocellis, A. Di Luccia, G. Marino, V. Di Marzo, Two novel classes of neuroactive fatty acid amides are substrates for mouse neuroblastoma "anandamide amidohydrolase", FEBS Lett. 377 (1995) 82–86.
[22] Y. Wang, F. Ramirez, G. Krishnamurthy, A. Gilbert, N. Kadakia, J. Xu, G. Kalgaonkar, M.K. Ramarao, W. Edris, K.E. Rogers, P.G. Jones, High-throughput screening for the discovery of inhibitors of fatty acid amide hydrolase using a microsome-based fluorescent assay, J. Biomol. Screen. 11 (2006) 519–527.
[23] S. Holt, J. Nilsson, R. Omeir, G. Tiger, C.J. Fowler, Effects of pH on the inhibition of fatty acid amidohydrolase by ibuprofen, Br. J. Pharmacol. 133 (2001) 513–520.
[24] M.P. Patricelli, H.A. Lashuel, D.K. Giang, J.W. Kelly, B.F. Cravatt, Comparative characterization of a wild type and transmembrane domain-deleted fatty acid amide hydrolase: identification of the transmembrane domain as a site for oligomerization, Biochemistry 37 (1998) 15177–15187.
[25] V. Di Marzo, T. Bisogno, T. Sugiura, D. Melck, L. De Petrocellis, The novel endogenous cannabinoid 2-arachidonoylglycerol is inactivated by neuronal- and basophil-like cells: connections with anandamide, Biochem. J. 331 (1998) 15–19.
[26] K. Ahn, S.E. Smith, M.B. Liimatta, D. Beidler, N. Sadagopan, D.T. Dudley, T. Young, P. Wren, Y. Zhang, S. Swaney, B.K. Van, J.L. Blankman, D.K. Nomura, S.N. Bhattachar, C. Stiff, T.K. Nomanbhoy, E. Weerapana, D.S. Johnson, B.F. Cravatt, Mechanistic and pharmacological characterization of PF-04457845: a highly potent and selective fatty acid amide hydrolase inhibitor that reduces inflammatory and noninflammatory pain, J. Pharmacol. Exp. Ther. 338 (2011) 114–124.
[27] U. Yapa, J.J. Prusakiewicz, A.D. Wrightstone, L.J. Christine, J. Palandra, E. Groeber, A.J. Wittwer, High-performance liquid chromatography-tandem mass spectrometry assay of fatty acid amide hydrolase (FAAH) in blood: FAAH inhibition as clinical biomarker, Anal. Biochem. 421 (2012) 556–565.